Maritime Sediments, Vol. 9, No. 2, September 1973, pp. 45-58.

Sediment Texture and Transport Studies in an Intertidal Environment: A Progress Report*

ROBERT W. DALRYMPLE
Department of Geology, McMaster University, Hamilton, Ontario

Introduction

Studies of subtidal sand bodies by a number of people (Houbolt, 1968; Klein, 1970, and references p. 1109; Caston, 1972, and Caston and Stride, 1970) have indicated that many sand-bars are characterized at least to some degree by an elliptical transport pattern around them. Klein (1970) believes that in his area, this is an equilibrium system as "both the sedimentary facies and morphology there has remained unchanged since 1947" (p. 1109). However, the presence of consistent, distinct areal variations in texture over this sand-bar poses a problem for a simple elliptical transport model.

The purposes of this research project thus are: first, to determine the paths of sediment transport in a tidally dominated sand-bar setting and to obtain values for the rates of transport and dispersion; secondly, to relate these observations to the hydraulic setting and thirdly, to attempt to interpret the textural and mineralogical distributions on the basis of the transport patterns and hydraulics.

1971 Data Analysis

Topographic Base Map: The survey data that was collected during June and early July of 1971 has now been synthesized into a topographic map of Selmah Bar (Fig. 1), with a 1-m contour interval. This map can now be used as a base for further work.

Megaripple Migration: One simple method of determining rates of sediment movement is to measure the migration of megaripples with respect to fixed stakes. Figure 2 gives some representative examples of these data.

Stakes 3 and 15 are located in the flood-dominated area of Selmah Bar. Here the respective rates of migration are: 16.5 cm and 25 cm per tidal cycle respectively, in the direction of the slip-face dip. The difference in the rates appears to be related to the current strengths. The maximum bottom-flood velocities near the stakes are: 65 cm/sec at stake 3, and 105 cm/sec at stake 15.

In many ebb-megarippled area however, the stake measurements do not show a simple migration pattern as was the case above. The data for stake 20 for instance, can be interpreted to show either flood (solid line) or ebb (broken line) migration. Current measurements do not resolve the problem. Although maximum bottom-flood velocities are 20 cm/sec higher than ebb velocities, the duration of ebb currents greater than 50 cm/sec exceeds that of flood currents. Depth-sounder records taken at high tide have shown that only flood megaripples are present then. This indicates that, in many areas where ebb megaripples are present at low tide, there is a continuous reworking and obliterating of the bedforms produced by the previous tidal cycle. Studies on bedform migration will be of little use in these areas.

Megaripple Wavelength-Amplitude Correlations: As a matter of interest, simple linear regression has been used to determine the degree of association between wavelengths and amplitudes of the megaripples on Selmah Bar. The log of both quantities was used and the resulting correlation coefficient was 0.52.

Despite the poor correlation, interesting trends emerge when the areal distribution of combinations which fall outside of one standard

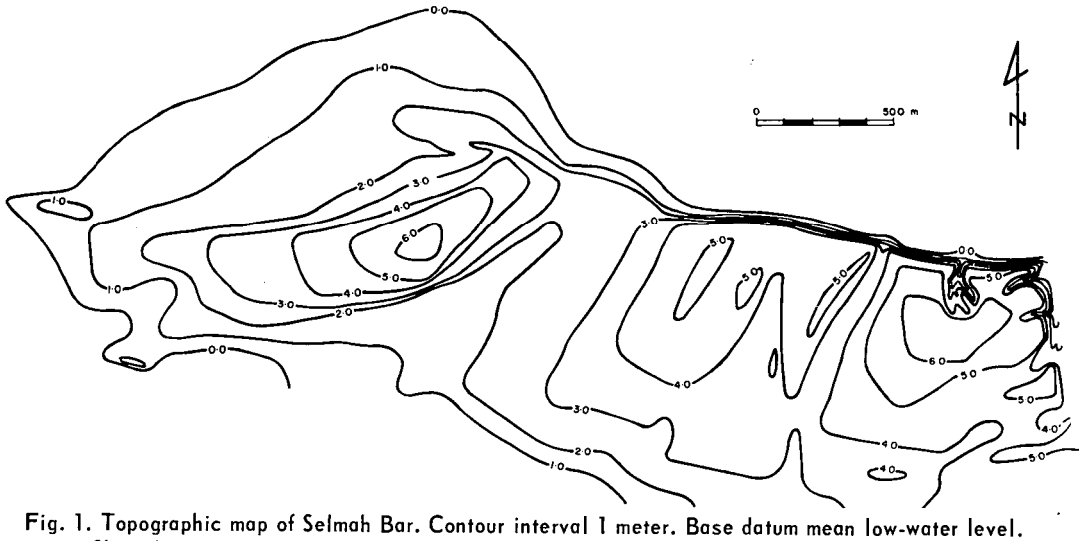

Fig. 1. Topographic map of Selmah Bar. Contour interval 1 meter. Base datum mean low-water level. Shore lies approximately 500 m south of the bar.

* Manuscript received December 20, 1973.

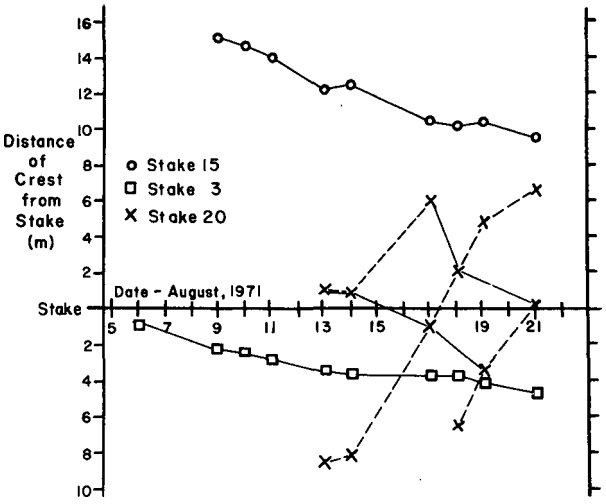

Fig. 2. Megaripple migration at selected stake locations, Selmah Bar. East (flood) is to the bottom on the distance axis, west toward the top.

deviation of the regression line is plotted (Fig. 3). In general, those points which plot more than one standard deviation above the line (amplitude too high for the wavelength) are derived from ebb megaripples. The largest number of the points that fall below one standard deviation (amplitude too low for the wavelength) are derived from the flood area. The latter exceptions are usually located on high, exposed portions of the bar, where wave activity often rounds off and lowers the megaripple profiles. The low amplitudes in the flood area might be due to ebb reworking. The excessive buildup of ebb megaripples in places could be the result of almost complete destruction of previously formed flood megaripples and the building of the ebb form on the back of the flood megaripple as mentioned above.

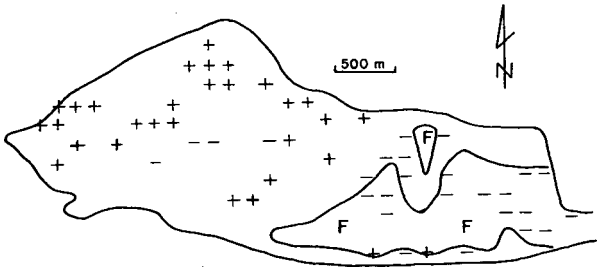

Fig. 3. Sample points falling more than one standard deviation from the regression line of log amplitude versus log wavelength (+ if amplitude too high for the wavelength; -- if amplitude too low for measured wavelength).

Graphic Textural Parameters: The graphic statistics of Folk and Ward (1957) have been calculated for the forty sieved samples from Selmah Bar. The sieve interval was .5ϕ. The geographic variations of these parameters are shown in Figure 4.

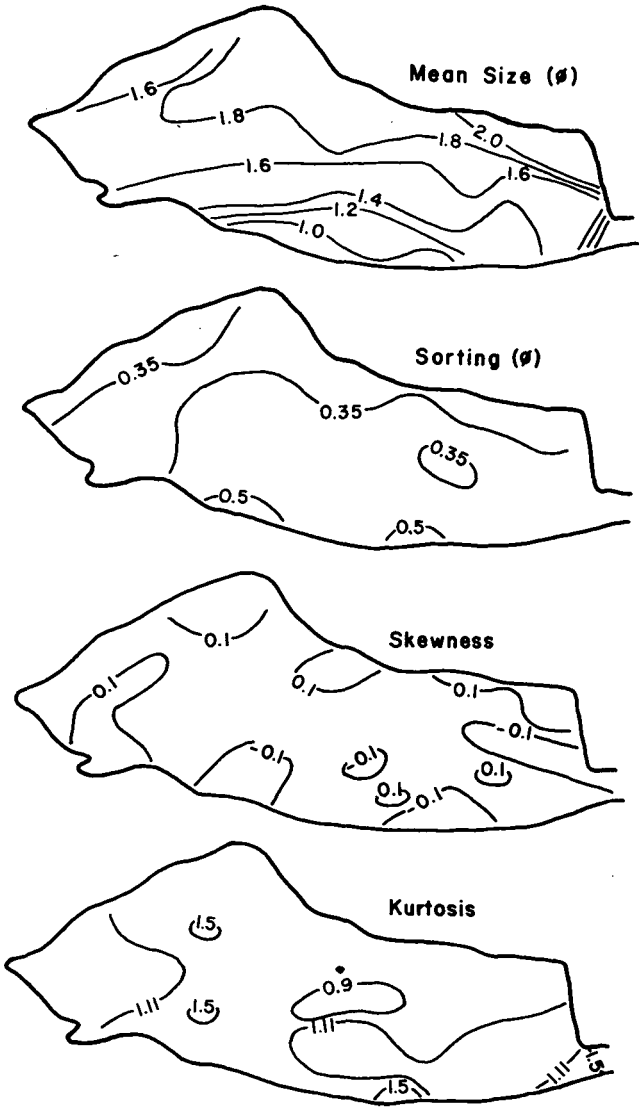

Fig. 4. Areal distribution of Folk and Ward (1957) grain-size statistics. Sorting, skewness and kurtosis contours are the verbal class limits: Sorting: under 0.35 -- very well sorted; 0.35 - 0.50 -- well sorted; 0.50 - 1.0 -- moderately well sorted. Skewness: -0.30 - -0.10 -- negatively skewed; -0.10 - +0.10 -- nearly symmetrical; +0.10 - +0.30 -- positively skewed. Kurtosis: 0.67 - 0.90 -- platykurtic; 0.90 - 1.11 -- mesokurtic; 1.11 - 1.50 -- lepokurtic; 1.50 - 3.0 -- very leptokurtic.

The contours of mean grain size tend to lie parallel to the length of the bar, with the coarsest sands lying nearest the shore. The finest material occurs at the eastern end of the bar and extends westward into coarser sand along the steep north side. Virtually all sands however, have their mean in the medium sand grade, as has been observed by Klein (1970, p. 1103).

The majority of the samples are well- to very well-sorted, with a trend toward increased sorting values as the mean size decreases. The best sorting occurs along the north side and west end of the bar, where current action is strongest and the input of coarser material from the shore is not felt.

The distributions of skewness and kurtosis are much more irregular. In general however, negatively skewed samples tend to be coarser and more poorly sorted than positively skewed samples. Kurtosis values do not follow any pattern that can be correlated with any of the other textural parameters. Most of the samples are mesokurtic to leptokurtic.

Areal Size Grade Variations: The percentages of the total sample retained on each sieve, from 0.0ϕ to 3.5ϕ, for each of the 40 samples have been plotted in order to undertake a more detailed study of the data contained in the sieve analyses (Fig. 5).

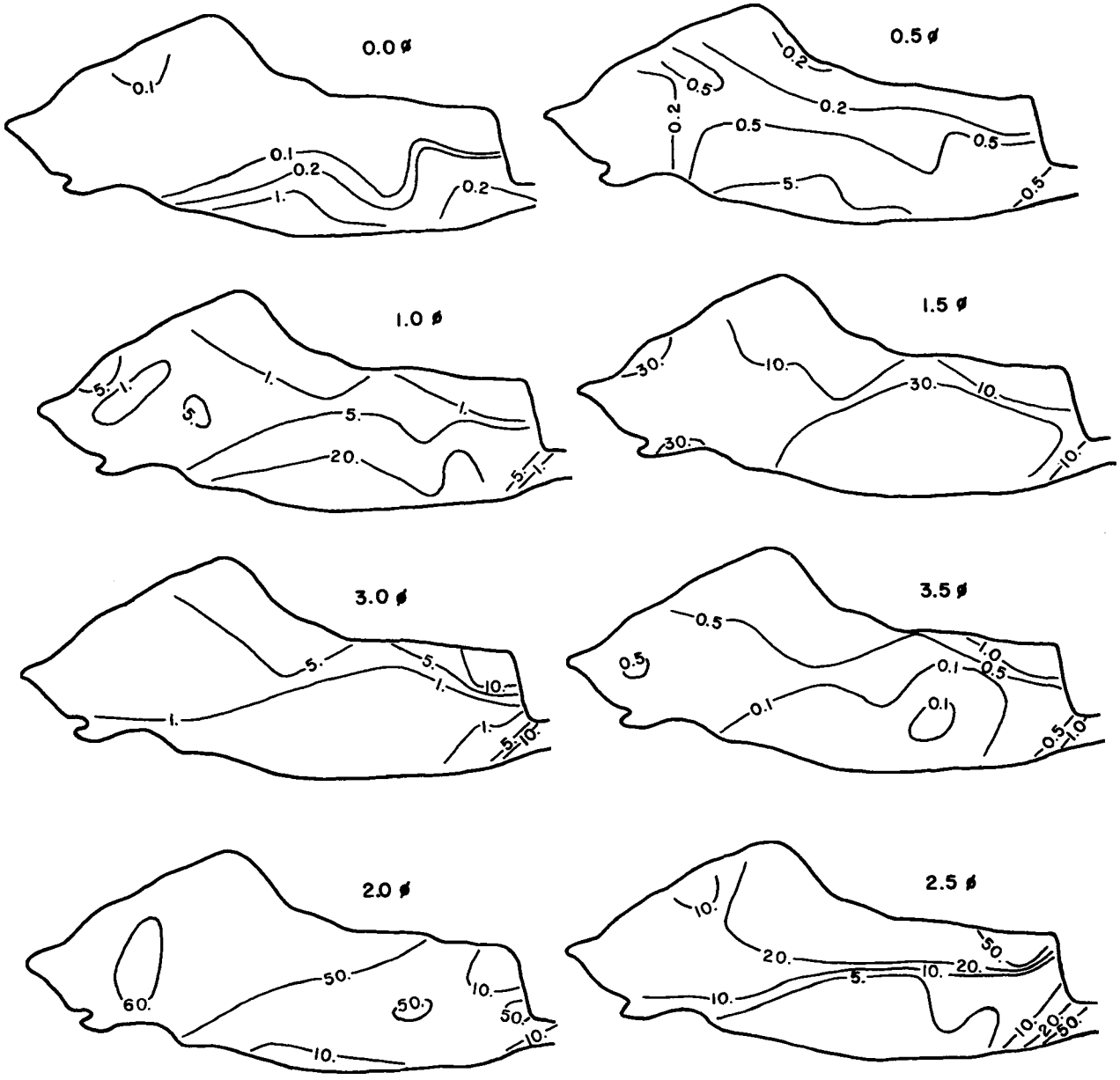

Fig. 5. Areal variation in weight percentage retained on the sieve of a given mesh size.

The distributional patterns that emerge are to be expected when the graphic statistics are considered. The highest concentrations of the coarse fractions, from 0.0ϕ up to and including 1.5ϕ are found nearest the shore. The amount of material retained on the 2.0ϕ sieve is almost of equal abundance everywhere, except immediately adjacent to the shore, and in the extreme east end next to the mudflats. In the finer sizes from 2.5ϕ to 3.5ϕ, the highest values are found across the extreme northern side of the bar and at the east end.

The contour patterns of Figure 5 and of the mean grain size indicate the presence of two main sand streams. The first involves the movement of coarse material, which appears to be derived from the shore, eastward along the south side of the bar in the flood area. This movement has a slight northward component and the sediment appears to be funnelled between the two areas of finer material at the eastern end of the bar. The second stream is a westward motion of fine material along the north side. This fine material, derived from the mudflats, is progressively diluted by coarser material to the west.

These two streams might be joined by northward flow in the tidal channel at the east end. However, if this does occur, the significant lack of material coarser than 1.5ϕ on the north side indicates that either this coarser fraction of the eastward moving stream is trapped further south, or there is sufficient lag in its rate of transport such that these grades have not yet reached the steep face.

A third minor stream moving coarser material northeastward up the low area cutting the centre of the bar is indicated by the doming of the contours in the north-central area on the 1.0ϕ-, 1.5ϕ-, 3.0ϕ- and 3.5ϕ-maps (Fig. 5).

A second small source of coarse sand might be present in the extreme northwest corner of the bar.

1972 Summer Field Work

In 1972, further field studies were conducted during June, July and August. Selmah Bar was the most intensely studied sand body again this year. Noel Bay Bar and East Noel Bar received more attention than in the previous summer however.

The investigations fall into three categories: 1) large-scale sampling to examine changes in textural variation from the previous field season; 2) sampling on a small scale to establish local textural differences between parts of megaripples; and 3) fluorescent tracer studies to determine the directions and rates of sediment dispersion.

Grid Sampling: In order to ascertain what, if any, textural changes had taken place on the sand bars over the course of the winter, all were resampled, but on a coarser grid than previously.

Selmah Bar was sampled on June 14, 15, 16, 21 and 22. Fifty-three samples were collected (Fig. 6), on a 300-m square grid, which had its origin in the vicinity of SB1 of 1971.

Eight samples were obtained from East Noel Bar, also on a 300-m square grid. These samples were collected on July 31.

The sampling on Noel Bay Bar was conducted on August 3. Fifteen samples were taken, one each from the crest area and from the gentle side, on lines varying from 250 m to 300 m apart.

As in 1971, all samples were from megaripple crests, to avoid local variations. Megaripple characteristics were not noted, as this aspect of the study was undertaken by John Knight (a fellow graduate student) on the same grid pattern.

As a strictly qualitative impression, it does not appear that any significant textural changes have occurred.

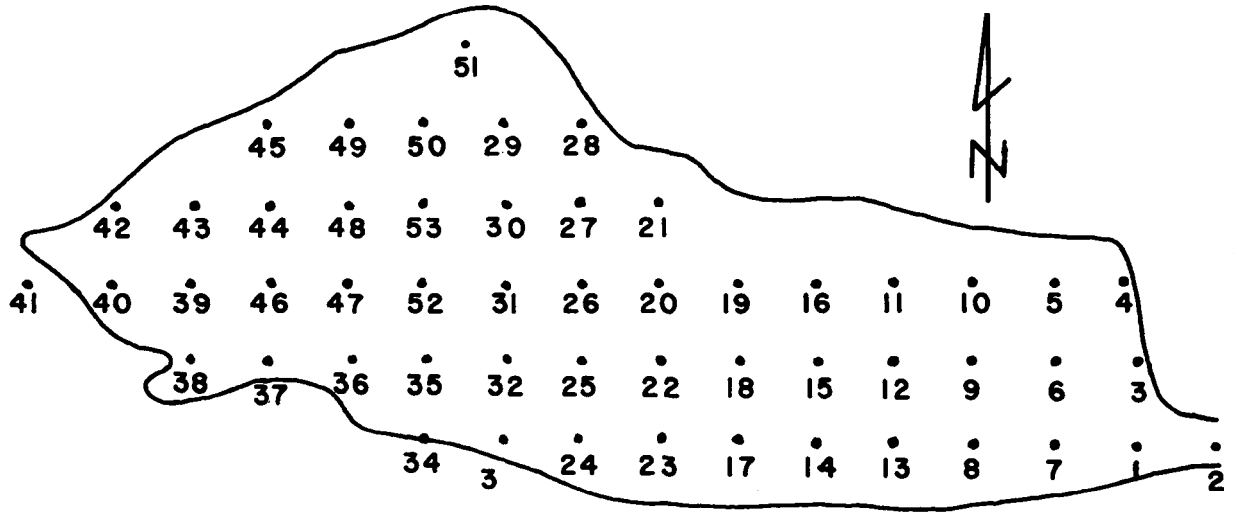

Fig. 6. Location of 1972 grid samples, Selmah Bar. Sample spacing 300 m.

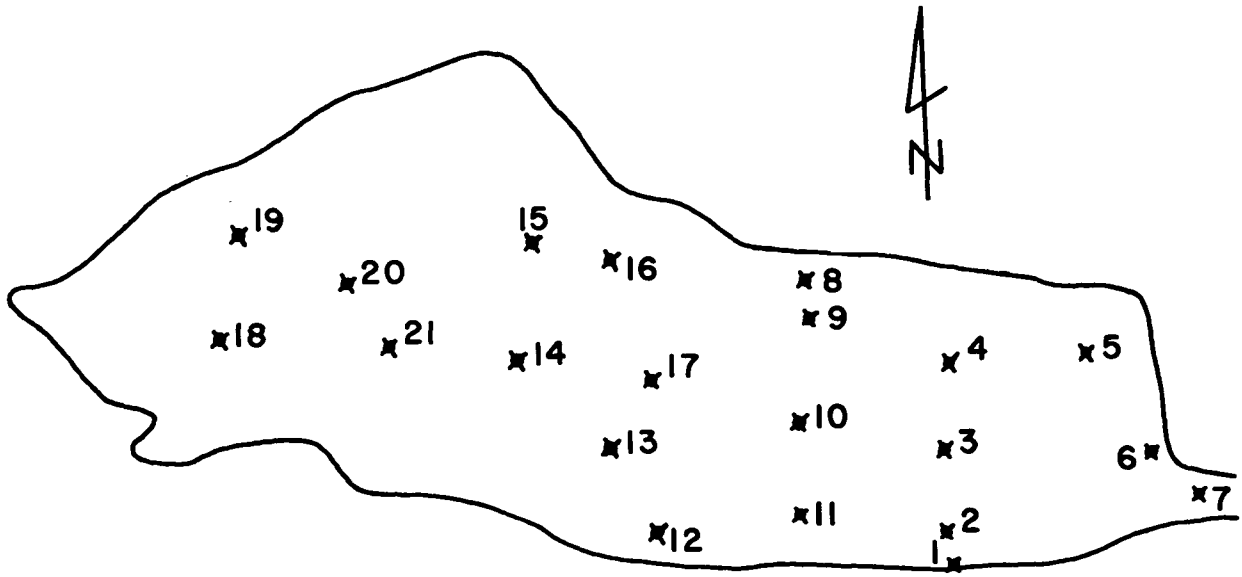

Fig. 7. Location of sample sites at which detailed sampling over megaripple profiles was conducted.

Textural Variations over Megaripples: In this phase of the study, samples were taken from the crest, trough bottom, and half way up the stoss side and slip face of a megaripple at twenty-one points dispersed over Selmah Bar (Fig. 7). All textural areas and megaripple types were included. The sampling was done on June 28, and July 5 and 6. As well as giving a better indication of all sediment present on the bar, the size variations should allow some inferences to be drawn regarding the hydraulics and the mechanics of sediment transport. It is also obvious that those sizes present in the troughs will move more slowly as they are buried for longer periods by advancing megaripples.

Fluorescent Tracer Studies: The use of fluorescent tracers provides an easy and inexpensive method of determining the pattern and rate of sediment dispersal. To the author's knowledge, only three studies have been made in similar or closely analogous situations. These are: Lüneburg (1960) on the sandy tidal flats of the German coast; Jolliffe (1963) on a tidally dominated sand bar off the Lowestoft harbour entrance, Great Britain; and Sandusky (1968) on Big Bar at Five Islands in Minas Basin, Nova Scotia. Other studies from estuarine tidal environments such as Blackley, Carr and Gleason (1972) exist, but in all cases, the

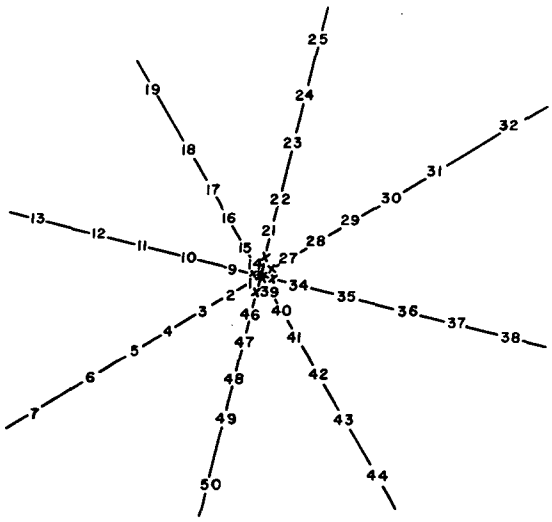

Fig. 8. Hypothetical sampling pattern for dispersal studies.

data are analyzed in only a summary fashion.

The coating mixture used in the present study is given approximately by Yasso (1966, p. 290, his formulation number 6). The amounts of materials used were: 3 cups of Day-Glo Acrylic Lacquer and 4 cups of Bettle Resin, diluted in 18 to 24 cups of toluene (acetone was used as a substitute for toluene in some cases). This was sufficient to coat 50 pounds of sand, the amount used in all dispersal trials.

The painting procedure involved the following steps: a) collection of the sand from the area in which the dispersal was to be monitored; b) drying of the sediment; c) mixing of the sand and paint solution with the aid of a portable cement mixer; d) drying of the painted sand; and e) disaggregation of any lumps formed during the drying period.

The coloured sand was then returned to the collection area. A shallow trench, 8 to 10 cm deep, 1 m by .5 m in size and oriented perpendicular to the crest was dug about half way up the stoss side of a megaripple. The tracer was placed in the trench and very lightly covered to prevent extremely rapid dispersal during flooding. A metal stake marked the centre of the dispersal site.

Sampling was usually conducted on one day (2 tidal cycles) after emplacement of the dyed sand, and again one week from the time of the first sampling. This schedule was followed for the five sites on Selmah Bar and the one on East Noel Bar. Due to weather and time considerations, the three stations on Noel Bay Bar were only sampled once, two days after injection.

In most of the collections, 50 samples were taken. A stellar pattern was used, with 8 rays drawn, 45° apart (Fig. 8). The initial ray was oriented perpendicular to the megaripple crest orientation. The grid radius did not usually exceed 40 m as experience indicated that the chance of finding fluorescent grains in the size of samples analyzed beyond this range was not very great. In all, approximately 775 samples were collected.

Most of the samples have now been analyzed. From each dried sample, 10 gm (usually) was separated and the number of fluorescent grains in it was counted. Based on a uniform grain size of 1.5ϕ to 2.0ϕ (the range of mean sizes) each 10-gm split contained between 150,000 and 520,000 grains. A 25-gm or 50-gm subsample was found to be too large for rapid processing. From these counts, contour maps of the dispersal at each station can be drawn (Fig. 14, 15, 16, 17, 18 and 20).

Two methods have been used in reducing the data. The first has been to calculate the average net transport distance (ANT). This is given by the equation:

$$ANT = \frac{\sum_{i=1}^{50} n_i d_i}{N}$$

where n_i = number of fluorescent grains in the i^{th} 10-gm sample, d_i = distance of the i^{th} sample from the origin and N = total number of fluorescent grains recovered. The distance given does not consider the directions of motion. This value should not be confused with the gross transport distance, which could theoretically be much greater.

The second technique has been to employ the vector mean (Potter and Pettijohn, 1963, p. 264) and weighted variations of it. In the unweighted case, the method computation is as follows:

$$V = \sum_{i=1}^{50} n_i \cos x_i \quad \text{and} \quad W = \sum_{i=1}^{50} n_i \sin x_i.$$

Therefore, the vector mean = $\bar{x}$ = arctan W/V, the resultant magnitude = $R = (V^2 + W^2)^{\frac{1}{2}}$ and the consistency ratio = L = (R/N)100, where: n_i and N are as above and x_i is the aximuth of the ray on which the i^{th} sample is located.

In many cases, the vector mean ($\bar{x}$) gave a reasonable approximation to the direction of preferred transport as inferred from the contour patterns. In some instances however (D1, first sampling for instance) a very large number of fluorescent grains found very close to the origin outweighed intermediate concentrations retrieved from greater distances in another direction. It was intuitively felt that the visual impression presented by the contour patterns represented the net direction of sediment transport. It was thus concluded that grains found at greater distances should be given a greater weighting than those close to the origin. On this basis, the above formulae were modified to:

$$V' = \sum_{i=1}^{50} d_i n_i \cos x_i \quad \text{and} \quad W' = \sum_{i=1}^{50} d_i n_i \sin x_i$$

where d_i = the distance of the i^{th} sample from the origin. The remaining equations are identical except for the substitution of V' and W' for V and W.

A third set of values has also been generated using the distances squared as weighting factors:

$$V'' = \sum_{i=1}^{50} d_i^2 n_i \cos x_i \quad \text{and} \quad W'' = \sum_{i=1}^{50} d^2 n_i \sin x_i,$$

etcetera.

(Throughout the remainder of the paper, a single prime (') will be used to denote quanities including a distance weighting, and a double prime ('') for those with a distance squared weighting.).

This last approach is justifiable since the intensity (areal concentration) of anything radiating from a point source decreases as the square of the distance from the source. The vector mean calculated in this manner usually gave quite agreement with the direction of movement indicated by the contour patterns.

Table 1 - Fluorescent Tracer Results, 1972

Station	Grains Recovered (per 10 gm)	Vector Mean Azimuths				Weighted, Standardized "Consistency Ratios"			Average Net Transport Distance (metres)
		$\bar{x}$ (degrees)	R (%)	$\bar{x}''$ (degrees)	$\bar{x}''$ (degrees)	R' (metres)	R'' $(metres)^2$	$\sqrt{R''}$ (metres)	
D1-1st	7000	209	41	139	103	1.1	4.0	2.0	1.2
-2nd	1430	110	53	94	96	2.5	13.0	3.6	2.0
D3-1st	1888	17	28	45	49	2.8	33.5	5.8	2.2
-2nd	84	67	78	62	61	12.2	237.	15.4	10.4
D4-1st	535*	100	21	176	200	18.0	1230.	35.1	16.0
-2nd	45**	342	49	312	273	13.3	570.	23.9	15.3
D5-1st	3396	77	82	85	92	2.3	12.1	3.5	2.2
-2nd	158	91	83	89	88	18.7	628.	25.1	16.5
D6-1st	1082	328	59	321	319	1.3	2.3	1.5	1.3
-2nd	105	273	33	269	269	6.0	42.8	6.5	3.5
D7	286	141	58	120	94	3.6	43.6	6.6	3.3
D8	431	185	58	173	177	3.2	14.1	3.8	3.4
D9	939	310	10	259	256	2.8	11.9	3.5	1.3

*-- based on 50 gm samples

**-- based on 25 gm samples

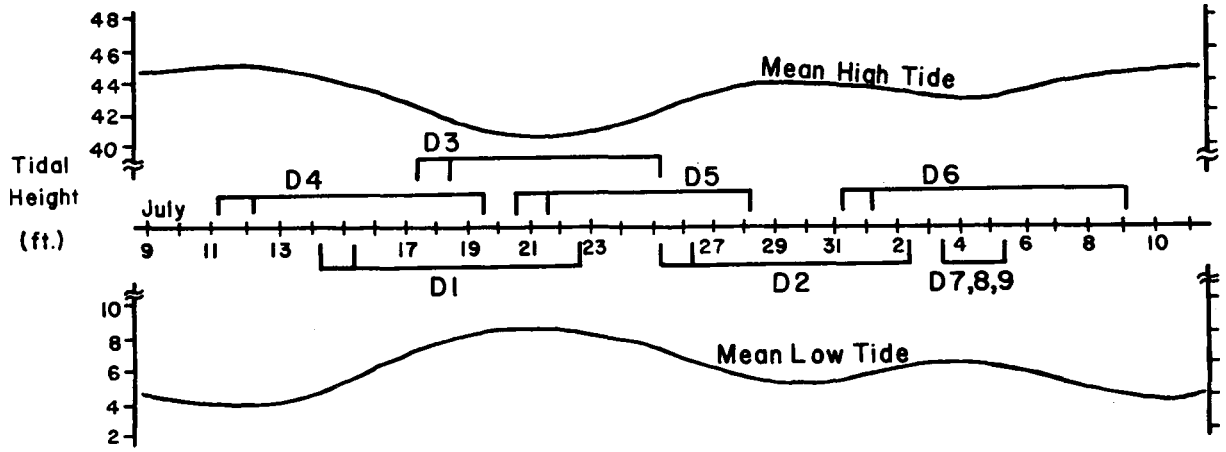

Fig. 9. Insertion and sampling dates of all tracer experiments and their position with respect to tidal range variations.

In the unweighted case, the consistency ratio is a measure of the dispersion only. When the distance is used as a weighting factor however, the scale on which the dispersion occurs also helps to determine the magnitude of this value. The consistency ratio could thus be used as a measure of the distance of transport if the dispersion factor could be removed. This can be done, as a first approximation, by dividing each weighted consistency ratio by the value of the unweighted consistency ratio. The dimensions of the two "consistency ratios" thus obtained also indicate that these ratios can be used as distance measures. R' (distance weighted) has the dimensions of length, and R'' (weighted by distance squared) those of length squared. To make R'' a measure of distance only, its square root has been used. All of the values obtained in these analyses are listed in Table 1.

Another point to be kept in mind during the discussion of the results is that they only cover a period of one week at each station and do not reflect the conditions at all times in the lunar cycle. As well, the time in the lunar cycle at which each test was run could not be standardized. Figure 9 gives the sampling dates and the duration of the test at each site in relation to the tidal range.

Dispersal stations D1 to D5 are located on Selmah Bar (Fig. 10). The sites have been chosen such that they lie in varied hydraulic settings and also allow the gross transport pattern on the bar to be evaluated. Each of these stations will now be discussed in turn, followed by those on the other two bars.

D1: Dispersal station D1 is situated in the flood-dominated area of the bar. The megaripples are large: wavelength approximately 15 m and amplitude, 60 to 80 cm. The crests are straight to sinuous. Some ebb-reworking of these flood megaripples is always present. The grain size is the coarsest of any of the sites occupied, with a mean size of 1.2 to 1.3ϕ. The currents, however, are the weakest. The maximum bottom velocity is in the flood direction with a value of 65 cm/sec.

The dispersal patterns obtained from the two samplings are given in Figure 11. They clearly show that sediment is being moved dominantly in the flood direction. The ray on which the maximum concentrations were found is rotated 45° clockwise from the ray perpendicular to the crest orientation however. After one week though, the pattern commences to swing northward.

The three vector means have been included on the dispersal patterns of all samplings. With those for the first sampling of D1, the affect of the distance weightings is clear. The unweighted mean azimuth of 208° is strongly influenced by a concentration of 3000 grains in a sample only 1 m from the origin on a bearing of 225°. The inclusion of the distance swings the resultant to 139°. When the distance squared is used, it swings even further to 103°, quite close to the orientation indicated by the contours. The results after one week support this latter vector mean as being a better representation of the preferred transport direction, since all three resultant azimuths lie between 90° and 110° at this time (Table 1).

During the interval of a week, several changes occurred. The very high concentrations of grains near the origin are no longer present, but a larger area has concentrations greater than 5 grains per 10 gm. This results from the dispersion of material which has taken place. However, the pattern has tended to resolve itself, with the preferred direction becoming more strongly developed, as evidenced by the increase from 40.7% to 53.2% in the unweighted consistency ratio.

Although the distance from the origin to the 5-grain contour has not expanded very much, the fluorescent grains have moved further from the origin on the average, after a period of one week. The enlarged areas inside the 5- and 10-grain contours points to this. Also, the average net transport distance (ANT) increased from 1.2 m to 2.0 m. Other indicators are the weighted "consistency ratios". R' increased from 1.1 m to 2.5 m and the square root of R'' from 2.0 m to 3.6 m.

D2: Dispersal station D2 is located near the base of the steep, north side of the bar. It lay between the steeper, plain bed area and the lower, flatter surface which is covered by wave-rounded, linguoid megaripples (Fig. 10).

Unfortunately the samples from this station have not been analyzed yet, since the mean grain size of 2.1ϕ meant that the sediment was too fine to allow unaided, visual counting of the fluorescent particles. A microscope will have to be used.

D3: This station was placed in the depression which trends from the shore north-eastward across the central portion of the bar (Fig. 13). The mean grain size here is 1.4ϕ to 1.5ϕ. Ebb megaripples with a wavelength of about 6 m and amplitudes of 30 to 50 cm are present. They indicate a flow in the direction of 225° to 240°. The dispersal patterns produced (Fig. 12) in this area however, indicate a transport direction almost 180° to this trend. In both cases, all three vector mean azimuths agree quite well with the visual contour impression. After one day they are: $\bar{x}$ = 17°, $\bar{x}$ = 48° and $\bar{x}''$ = 49°. After a week they become: $\bar{x}$ = 67°, $\bar{x}$ = 62° and $\bar{x}''$ = 61° (Table 1).

The reason for the apparent discrepancy between the megaripple and tracer pattern orientations is the same as that presented above while discussing the bedform migration studies. Current measurements show that the maximum ebb-bottom velocity is only 65 cm/sec, compared with a flood speed of 100 cm/sec. Thus, flood currents dominate. The ebb bedforms are the result of complete reworking of the flood features which are present at high tide.

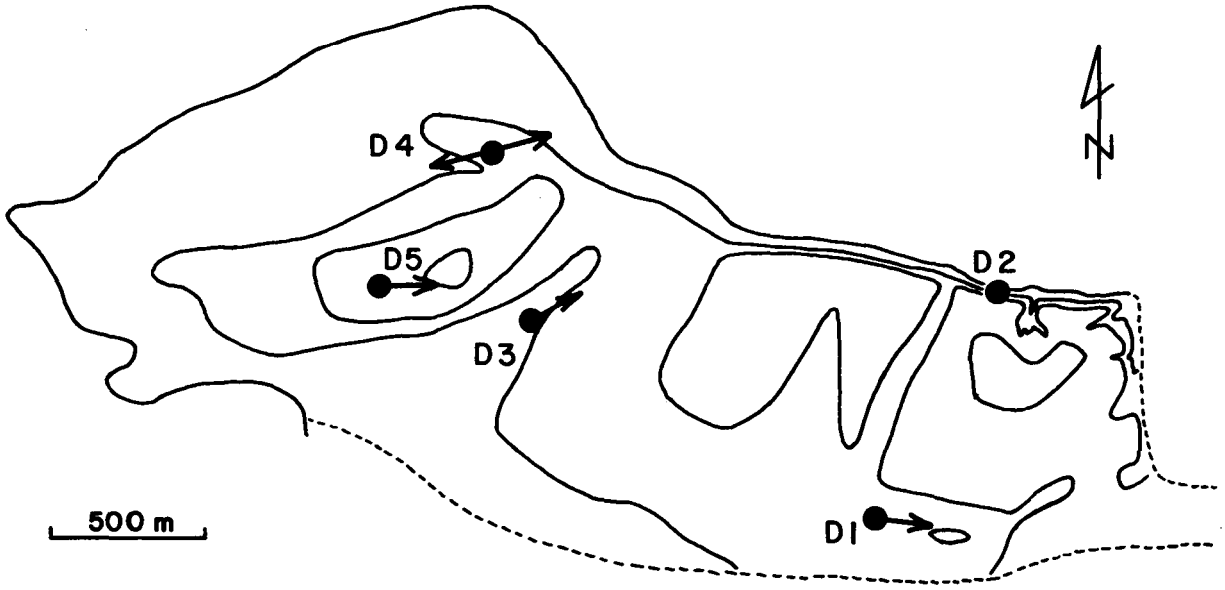

Fig. 10. Selmah Bar showing location of tracer dispersal sites. Arrows give the resultant transport direction as indicated by the distance squared weighted vector mean. No well defined net transport direction was obtained at D4.

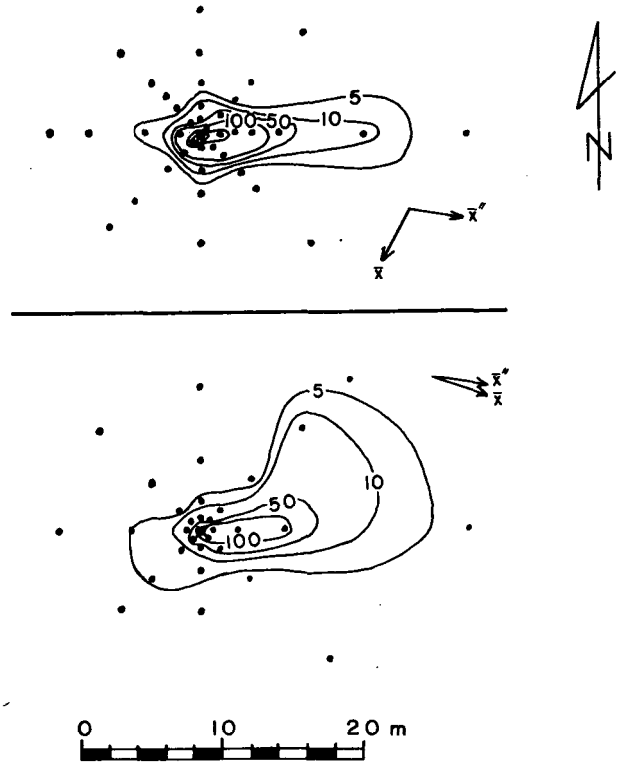

Fig. 11. Dispersal station D1: Contours in number of fluorescent grains counted in a 10 gram sample. Dots are sample points. Origin marked by cross. Arrows are vector means (see ntext for details.) Unlabelled contours are multiples by 10 of 5 and 10. Top: 1 day after injection; Bottom: 8 days after injection.

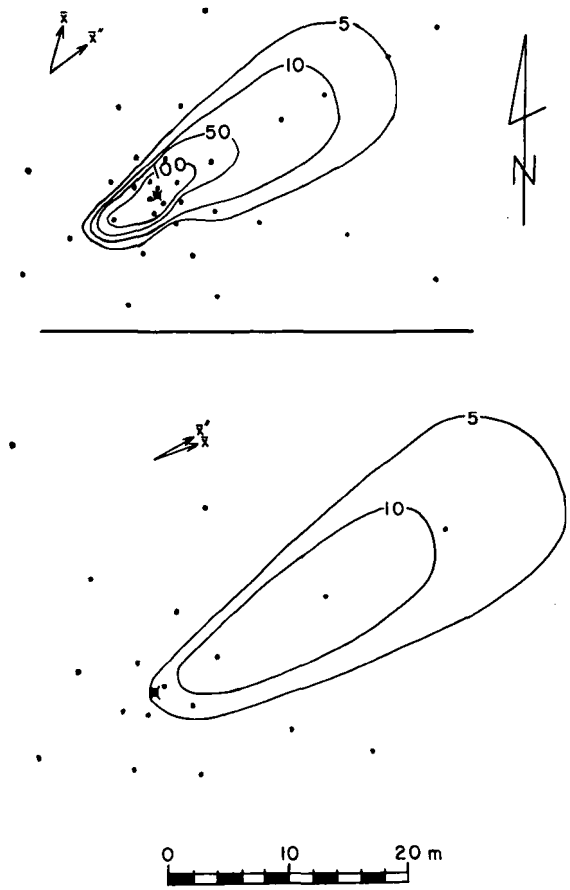

Fig. 12. Dispersal station D3: All notation as on Figure 11. Top: 1 day after injection; Bottom: 8 days after injection.

The distances of transport here are considerably larger than at D1, as would be expected from the higher maximum current speeds. For the first and second samplings, the respective values of ANT are 2.2 m and 10.4 m. The weighted "consistency ratios" are: R' = 2.8 m and 12.2 m and the square root of R'' = 5.8 m and 15.4 m (Table 3). The rate of increase of ANT between the two samplings is also much larger here than at D1, a result probably of the more intense reworking.

D4: D4 is located (Fig. 10) on a spur of the main crest, on the exposed, north-central portion of the bar. Large ebb megaripples with wavelengths of about 7 m and amplitudes ranging from 50 cm to 1 m are exposed at low tide. The mean grain size is 1.9ϕ.

This station is subjected to the highest currents measured anywhere on the bar, because of its exposed position. As has been stated above, neither flood nor ebb currents clearly dominate. Both the high current strengths and the lack of a dominant current are reflected in the dispersal pattern obtained after the occurrence of two tidal cycles (Fig. 13).

From the data of one day following the injection, the unweighted mean resultant azimuth was 100°, influenced by the higher concentrations to the east of the centre. The distance weighted value was 176° and $\bar{x}''$ was 200°. This latter value reflects the greater distances at which concentrations greater than 5 grains occur to the west. The very low consistency ratio of 21% is caused by the extremely bimodal nature of the transport.

After an interval of one week, the very rapid dispersion of material has all but reduced the concentrations of fluorescent particle below the limit of detection. The dispersion is still high as the consistency ratio is only 49%, but this is an improvement. The mean azimuths now lie between north-northwest ($\bar{x}$ = 342°) and almost due west ($\bar{x}''$ = 273°). To what extent this represents a preferred westerly transport is not known.

Unfortunately, the area within the contours and the various distance measures for D4 cannot be compared with any of the other sites. The grain counts used in the first sampling are based on sample splits of 50-gm and in the second sampling, on 25-gm samples. Thus, everything is larger for D4. The decrease in the weighted "consistency ratios" for the second sampling from the first could be the result of the smaller sample size at one week's time.

D5: Dispersal station D5 is situated on the western portion of the main crest. The mean grain size is just less than 1.6ϕ. The bedforms in the area are small ebb megaripples with wavelengths of 3 to 4 m and amplitudes of 20 to 30 cm.

The situation at D5 is similar to that at D3. The ebb bedforms do not indicate ebb dominance, but only transient features which are destroyed by the flood tide. It is common to see the remains of the stoss side of a flood megaripple protruding below the ebb slip face.

The current measurements show a flood maximum of 90 cm/sec as compared with an ebb maximum of only 65 cm/sec. This combined with the incomplete reworking of the flood megaripples suggests the presence of a flood-oriented, net-transport direction.

The pattern produced by the tracer concentrations (Fig. 14) supports this interpretation. After both a day and a week, the contours show almost unidirectional transport to the east. The vector mean azimuths are also very similar. In the first case they lie between 77° and 92°. For the one-week pattern, the spread is only 3° and lies between 88° and 91°. The unweighted consistency ratios also reflect this with values of 82% and 83% (Table 1).

Of all the stations from which the results can be compared, this location showed the greatest transport after a period of one week. The values of ANT are 2.2 m and 16.5 m. The weighted "consistency ratios" are: R' = 2.3 m and 28.7 m and $\sqrt{R''}$ = 3.5 m and 25.1 m (Table 1).

The significant increase in all of these values between the two samplings is of interest. For the average net-transport distances, the increase from 2.2 m to 16.5 m is 7.5 times in magnitude. It might be expected that the transport would be quickest at first, due to the exposed position of the tracer, with a decrease as time passed and the tracer became mixed. At both samplings however, the given value of ANT represents a distance of 1.1 m per tidal cycle. This constant transport rate can be explained in several ways. First of all, the transport rate could indeed be constant. Secondly, the positioning of the tracer initially on the stoss side of an ebb megaripple would shield it partially from the first flood current. Thus, the transport rate at one day might be low. Thirdly, the emplacement was done at neap tide, but after a period of one week, the tidal range was very nearly at spring tide. This might have increased the transport rate, thus offsetting any tendency for it to decrease with time.

D6: D6 was the only dispersal station occupied on East Noel Bar. It was situated nearer the outer edge, in medium sand. The ebb megaripples there have wavelengths of 3 to 5 m and amplitudes of approximately 25 cm.

The current measurements from the vicinity of this station show an ebb dominance. The flood current briefly achieves a maximum bottom velocity of 85 cm/sec. Although the ebb current does not reach as high a speed, it remains at velocities greater than 50 cm/sec for periods almost four times as long as the flood tide.

This ebb dominance is shown in the tracer patterns (Fig. 15). The vector mean azimuths after a period of one day ($\bar{x}$ = 328° and $\bar{x}''$ =

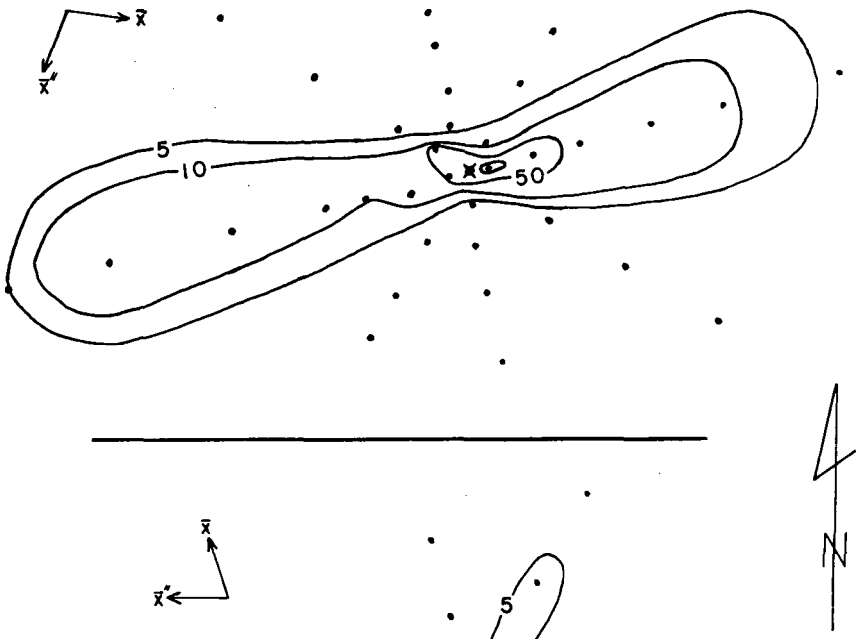

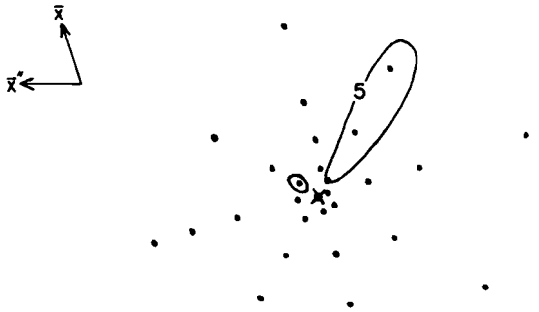

Fig. 13. Dispersal station D4: Dots, crosses and arrows as on Fig. 11. Top: 1 day after injection. Contours in number of fluorescent grains in 50 grams; Bottom: 8 days after injection. Contours in fluorescent grains in 25 grams.

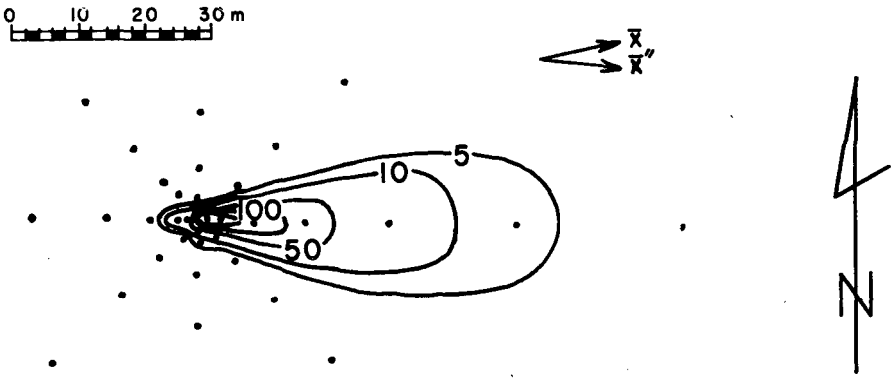

Fig. 14. Dispersal station D5: All notation as on Figure 11. Top: 1 day after injection; Bottom: 8 days after injection.

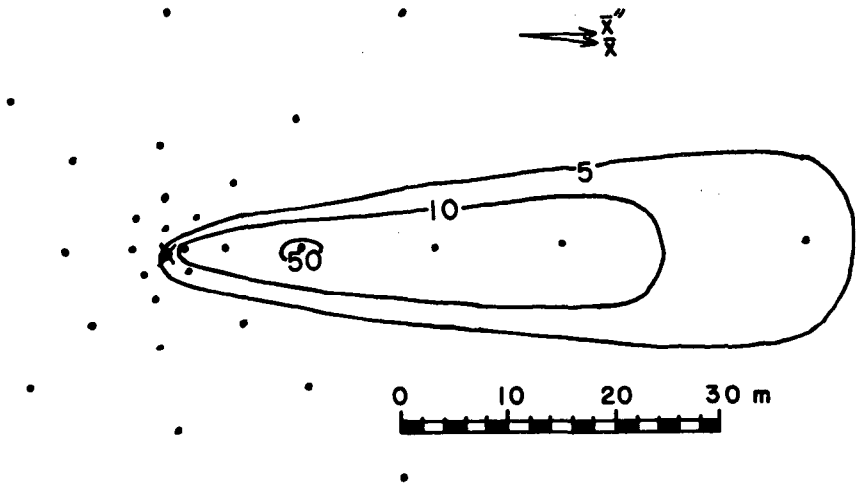

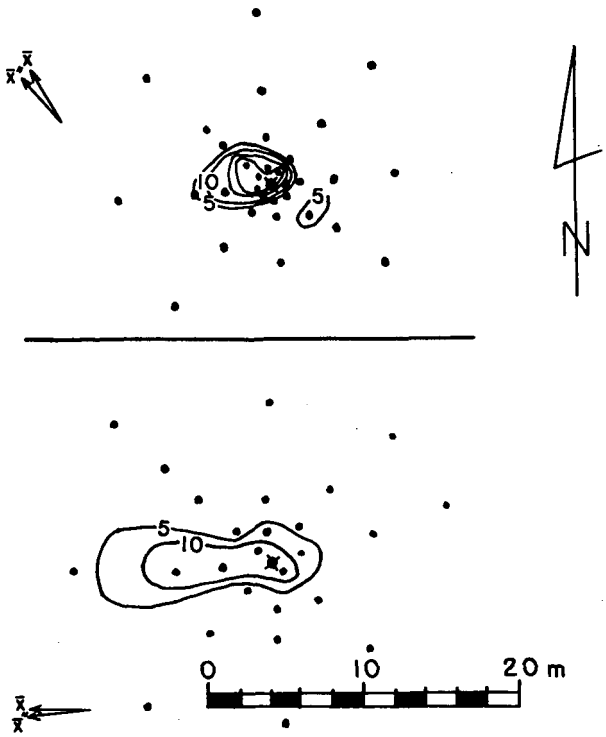

Fig. 15. Dispersal station D6 (East Noel Bar). All notation as on Figure 11. Top: 1 day after injection: Bottom: 8 days after injection.

319°) and after one week ($\bar{x}$ = 273° and $\bar{x}''$ = 269°) do not deviate much from each other despite the relatively high dispersions (59% and 33%).

The distances of transport (Table 1) here are low as would be expected from the weak current strengths. Both transport distances and currents are only a little greater than at D1.

D7: This dispersal station, as well as D8 and D9, are located on Noel Bay Bar (Fig. 16). D7 was situated on the steep, smooth, south face of the bar. No bedforms are present here. The sediment all over the bar is medium to fine sand.

Unfortunately, no detailed current measurements are available at this time for any of these stations. Also, since the sampling was conducted after two tidal days, the contour patterns obtained (Fig. 20) are not directly comparable with those from the other bars.

The sediment movement at D7 (Fig. 20A) is in a flood direction with a down-slope component. The vector mean azimuths, as expected, fall in the southeast quadrant (Table 1). The down-slope component here is unexpected though. In order for the bar crest to be maintained, there should be converging flow at the crest. It is possible that wave attack has moved material down-slope during the course of the study.

If the various distance measures are calculated (Table 1) on a daily or tidal cycle basis, they are very similar to those at any of the other dispersal sites on Selmah or East Noel bars.

D8: This station was on the gently sloping, north surface of the bar. Ebb megaripples are present here at low tide and are small to intermediate in size (wavelengths = 3-4 m, amplitudes = 20 cm). On the day of sampling, they were very wave-washed and rounded because of the considerable wave action in the area during emergence. This wave activity, from the northwest, might be a factor in producing the strong up-slope movement of sediment recorded (Fig. 17B). In the calculations of the vector means, the nearly symmetrical east and west extensions cancel and only the southerly motion is reflected.

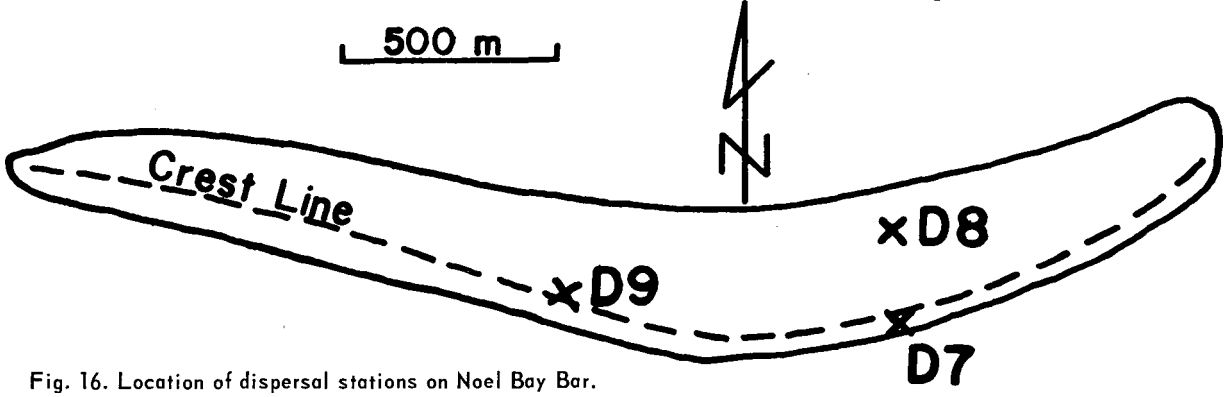

Fig. 16. Location of dispersal stations on Noel Bay Bar.

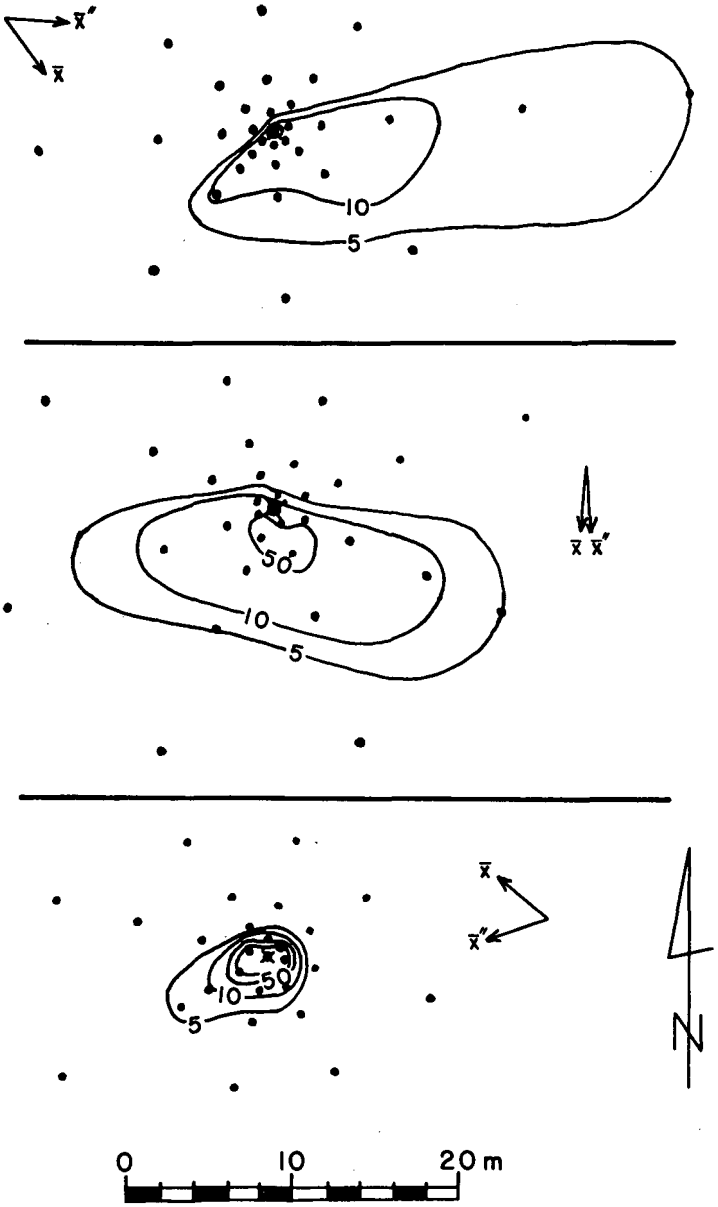

Fig. 17. All notation as on Figure 11. Sampling conducted two days after injection. Top: Dispersal station D7; Middle: Dispersal station D8; Bottom: Dispersal station D9.

If an elliptical, "race-track" sediment transport model exists on Noel Bay Bar, this area should be ebb dominated to compliment the flood area at D7. To what extent the results at D8 support or refute this model cannot be evaluated at this time.

The distance values for D8 are quite similar to those at D7. The identical 58% for the unweighted consistency ratios is another point of similarity in the sediment motion at these two stations.

D9: Dispersal point D9 was situated right on the crest of the bar in an area of large ebb megaripples. Wavelengths were about 4 to 5 m and amplitudes reached 80 to 100 cm.

The movement of sediment here (Fig. 17C) is the slowest of any point monitored on any of the bars. The preferred direction is ebb ($\bar{x}$ = 310° and $\bar{x}''$ = 256°), but the degree of preference is very slight as shown by the unweighted consistency ratio of only 10%. The distance measures (Table 1) are also very low, being less than half of the values for dispersal station D1.

This very slow rate of sediment motion and lack of any dominant movement direction could indicate that the crest area is a meeting point of sediment streams moving in opposite directions. No firm conclusions can be drawn yet.

Acknowledgements

The author would like to express his appreciation to R. John Knight for his assistance and helpful discussion while in the field. Much of the fluorescent tracer data would not be available but for the diligence and long-suffering of Tak-Chi (Mike) Yu, who performed most of these grain counts. Also, Mr. and Mrs. Ivan Main are thanked for their many kindnesses over the summer.

This work has been carried out while the author was the recipient of a National Research Council 1967 Science Scholarship and under the supervision of Dr. G.V. Middleton, McMaster University.

References Cited

BLACKLEY, M.W.L., CARR, A.P., and GLEASON, R., 1972, Tracer experiments in the Taw-Torridge estuary with particular reference to Braunton Burrows NNR: Unit of Coastal Sedimentation, Taunton, England, Report No. UCS 1972/22, 19 p.

CASTON, V.N.D., 1972, Linear sand banks in the southern North Sea, Sedimentology, v. 18, p. 63-78.

_____, and STRIDE, A.H., 1970, Tidal sand movement between some linear sand banks in the North Sea off Norfolk: Marine Geol., v. 9, p. M38-M42.

FOLK, R.L., and WARD, W.C., 1957, Brazos River bar: a study in the significance of grain size parameters: Jour. Sed. Pet., v. 27, no. 1, p. 3-26.

HOUBOLT, J.J.H.C., 1968, Recent sediments in the southern bight of the North Sea: Geol. en Mijnbouw, v. 47, no. 4, p. 245-273.

JOLLIFFE, I.P., 1963, A study of sand movement on the Lowestoft sandbank using fluorescent tracers: Geog. Jour., v. 129, no. 4, p. 480-493.

KLEIN, G. deV., 1970, Depositional and dispersal dynamics of intertidal sand bars: Jour. Sed. Pet., v. 40, no. 4, p. 1095-1127.

LUNEBURG, von H., 1960, Sedimenttransport, sedimentation und erosion auf den Aussensanden der Wesermündung: Report, 21st International Geol. Cong., pt. XXIII, p. 19-25.

SANDUSKY, C.L., 1968, Sand distribution from a point source: Unpub. Report, Advance Science Seminar on Intertidal Zone Sedimentation, 16 p.

YASSO, W.E., 1966, Formulation and use of fluorescent tracer coatings in sediment transport studies: Sedimentology, v. 6, p. 287-301.